DEVELOPMENT AND CHARACTERIZATION OF PROTRANSFERSOMES LOADED WITH MODEL DRUG FOR TRANSDERMAL DELIVERY

Hatem M. Tawfek[1,3*], Mohamed A. Nasr-Eldin[3,4], Mohamed A. Akl[2], Mohamed El-sayed[1], Ahmed R. Gardouh[1]

[1]Department of Pharmaceutics and Industrial Pharmacy, Faculty of Pharmacy, Suez Canal University, Ismailia, 41522, Egypt

[2] Department of Pharmaceutics and Pharmaceutical Technology, College of Pharmacy (Boys), Al-Azhar University, 1 El-Mokhayam El-Daem St., Nasr City, P.O. Box 11884, Cairo, Egypt.

[3] Military Medical Academy

[4] Armed Forces Pharmaceutical Factory

***Corresponding author:** E.mail: hatemmohamedtawfek@yahoo.com

ABSTRACT

Repaglinide (REP) is an oral synthetic antidiabetic that is administered to enhance meal-induced insulin production. It is quickly excreted from the body through the biliary system. Due its first-pass metabolism that occurs in the liver, REP has a low oral bioavailability of 56%. Its half-life in systemic blood circulation is approximately one hour, and it has a high plasma protein binding (greater than 98%). In addition to having a high lipophilicity (log P = 3.97) and extremely low water solubility (34 µg/mL at 37°C), REP also has a low and inconsistent bioavailability. The objective of this study was to develop a nanocarrier system called protransfersomes loaded with repaglinide REP-PTFs that provides the benefits of prolonged drug release and enhanced its bioavailability. Fabrication of REP loaded protransfersome nanovesicle by using different types of surfactants (tween 80, span 60, poloxamer188, and their combinations). All six different REP-PTF NVs formulations with different edge activator were prepared and characterized by measurements of Particle size (PS), polydispersity index (PDI); Zeta potential analysis (ZP) and % Entrapment efficiency (EE) were used as input parameters in Rank order to find the most optimal REP-PTF NVs composition. The results demonstrated that altering the type of surfactant had a significant impact on the Particle size (PS), polydispersity index (PDI); Zeta potential analysis (ZP) and % Entrapment efficiency (EE) of the REP-PTFs. The average particle size varied between 184.7 ± 9.7 and 629.7 ± 172.5 nm. The particles exhibited a negative charge, with zeta potential values ranging from −37.77 ± 1.77 to −29.1 ± 1.03 mV. The % E.E varied between 78±4.9 and 95.8±3.2 %. REP-PTFs exhibited prolonged drug release compared to the dissolution of REP suspension. Topical application of protransfersomes onto the abdominal skin of hairless mice resulted in better drug absorption than REP free. In conclusion, these results suggested that protransfersome has the potential to deliver REP via transdermal routes.

Keywords: Repaglinide (REP), Protransfersomes (PTFs), Transdermal delivery system (TDD), Bioavailability.

Introduction

Transdermal delivery system TTD is a highly effective pathway for the distribution of a drug throughout the body's circulatory system. The reason for this is the extensive surface area of the skin, which allows for convenient access and several choices for the absorption of substances through the skin. Moreover, medications exhibit more consistent pharmacokinetic profiles with less occurrence of peaks, hence reducing the likelihood of hazardous adverse reactions. This strategy not only enhances patient adherence by reducing the frequency of dosing, but it is also appropriate for patients who are unconscious or experiencing vomiting, as well as those who depend on self-administration ***(Ita, 2014)***.

TDD enhances bioavailability by circumventing pre-systemic metabolism. Nevertheless, the ability of medication molecules to pass through the skin is hindered by the protective layer of human skin epithelium, which acts as a barrier against external chemicals ***(Ramkanth et al., 2018)***. In recent times, a range of techniques have been employed to enhance the transdermal distribution of active medicinal components such as liposomes, niosomes, elastic liposomes (ethosomes), and transferosomes. Transferosomes, among other strategies, have the ability to easily change their shape under external force and can penetrate deep into the epidermal layers with high water content, ultimately reaching the subcutaneous tissues. Unlike traditional liposomes, transferosomes have the ability to transport large molecules, such as proteins, through the bloodstream ***(Rajan et al., 2011)***.

Transport of the drug through skin is best route of drug delivery because the skin is largest organ in human body. Drug carries which are used in transdermal drug delivery such as liposomes, niosomes, or microemulsions pose a problem that they remain mostly confined to the skin surface and therefore do not transport drugs efficiently through the skin. Because of the deformable nature of transfersomes, it penetrates through the pores of stratum corneum which are smaller than its size and get into the underlying viable skin in intact form. Vesicle shape and size, entrapment efficiency, degree of deformability, number of vesicles per cubic mm can be characterized by in vitro studies. Thus, they act as a carrier for low as well as high molecular weight drugs e.g. analgesic, anesthetic, corticosteroids, sex hormone, anticancer, insulin. The transdermal drug delivery system overtakes the pitfall associated with oral drug delivery system. It decreases the dosing frequency, diminish the GI based side effect by avoiding the first pass metabolism and enhances patient compatibility ***(Pandey et al., 2018)***.

Transfersomes (ultra-deformable vesicles) are the first generation of elastic, soft malleable vesicles which are tailor-made for enhanced delivery of active agents through the skin. These are special type of liposomes composed of phospholipids and an edge activator, which destabilize lipid bilayers and increase the deformability of the vesicles making them more compliant to penetrate through intact skin. Along with its ability to accommodate hydrophilic drugs, transfersomes possess elasticity of several orders more than the standard liposomes enhancing skin penetration ***(Nirwan et al., 2021)***. Conventional liposomes have nominal penetration across stratum corneum (SC), that tends to accumulate over the surface delivery insignificant progress in the treatment of

osteoporosis ***(Zheng et al., 2020)***. In contrast, transferosome are suitable for controlled and targeted drug delivery because of their ability to exhibit characteristics associated with cell vesicles ***(Patnaik et al., 2021)***. However, the problem of these ultra-flexible vesicles is self-stability. Therefore, to enhance the stability of these vesicles, use of liquid crystalline, pro-ultraflexible lipid vesicles (protransfersomes) has been proposed. Protransfersomes have the ability to get converted into ultra-flexible lipid vesicles (transfersomes) in-situ, upon absorbing water from the skin ***(Gamsjaeger et al., 2021)*** .

Protransfersomes exhibit superior entrapment efficiency and are suitable for incorporating both lipophilic and hydrophilic medicines, while also providing improved stability. Due to the characteristics of protransfersomes, such as their capacity to accommodate and improve the skin penetration of lipophilic substances, these molecules can serve as a good vehicle for delivering medications that have poor penetration abilities ***(Khatoon et al., 2019)***. The fluidic characteristic of protransfersomes restricts its application to the surface of the skin. Therefore, employing a vehicle for its transportation can yield advantageous outcomes. Khatoon et al. conducted a study on the transdermal application of clinidipine loaded transfersome gel. The study found that the gel had a higher entrapment efficiency and did not cause any hazardous effects. This conclusion is supported by previous studies conducted by ***(Srivastava et al., 2021)***.

Diabetes mellitus is a widespread, persistent ailment with serious life-threatening results on different parts/functions all over the body. The maximum number of diabetic sufferers is observed to be type II diabetes mellitus, i.e., (non-insulin-dependent). To control this type of diabetes, various classes of oral anti-diabetic drugs are commonly utilized in the market to decrease dosage and adverse effects accompanying the drug. Belongs to this various medications available from different classes being utilized, such as Sulfonylurea Thiazolidinedione, Biguanide Meglitinide analogs, and Glucosidase inhibitors etc. ***(Ebrahimi et al., 2015).***

REP is an oral medicament utilized to treat type 2 diabetes; belongs to Biopharmaceutical Classification System Class II. It is absorbed rapidly in the gastrointestinal tract (GI) and has a high hepatic first pass effect with a mean bioavailability of about 50–60%. It is eliminated fast from the body by the biliary excretion route. Its mechanism of action is partially like sulphonylureas like glibenclamide which stimulates the release of insulin from the pancreatic beta cells by closing ATP-dependent potassium channels in the presence of glucose. The half-life of REP is about 1 h, so it should be used 3–4 times in a day ***(Nasr-Eldin et al., 2024; Pandey et al., 2020)***. For bioavailability enhancement of REP, the researchers have attempted various approaches to overcome the challenges associated with oral delivery of Repaglinide, such as nanoemulsions, self-nano emulsifying systems, nanocrystals, solid lipid nanoparticles, nanostructured lipid carriers **(Nasr-Eldin *et al.*, 2024)** and protransfersomes **(Kesharwani et al., 2022)**.

Experimental

Materials

Repaglinide, Lutrol®F68, Lutrol®F127, Carboxymethyl cellulose (CMC), Span 80 (S80) and Tween 80 were kindly gifted by Egyptian International Pharmaceutical Industrial Company (EIPICO) (Egypt). Lipoid Phospholipon®90G (Phosphatidylcholine (PC) from soybean lecithin) was kindly provided by Lipoid GmbH (Ludwigshafen, Germany). Membrane filter (0.45 µm) Millipore purchased from Sigma Aldrich (USA). Propylene glycol was purchased from Morgan Chemical Company, Egypt. Solvents (distilled water, methanol) of HPLC analytical grade were purchased from Fisher Scientific Company (USA). Potassium phosphate monobasic was purchased from Alpha Chemika (India). Ethanol absolute (HPLC grade) was purchased from Merck (Germany). Alloxan, Formalin, and Hematoxylin stains purchased from Sigma Aldrich (USA). All other chemicals were used of analytical grade.

UV-scanning of REP

To measure REP's UV spectrum in methanol solution, the material was precisely weighed to 10 mg and then put into a 200-ml volumetric flask filled with methanol. The 50 µg/ml solution was stored in a cuvette. A UV visible spectrophotometer (Shimadzu, model UV-1800 PC, Kyoto, Japan) was used to record the UV spectra in the 200–400 nm wave length region in comparison to a blank methanol solution ***(Nasr-Eldin et al., 2024)***.

Construction of calibration curve of REP in methanol

The least amount of methanol was used to dissolve 50 mg of (REP), and the volume was increased to 1000 ml using methanol (stock solution). Solutions containing 2.5, 5, 7.5, 10, 12.5, 15, 17.5, 20, 22.5, and 25 µg/ml were obtained by adding 10 ml of methanol to samples of 0.5, 1, 1.5, 2, 2.5, 3, 3.5, 4, 4.5, and 5 ml. Using methanol as a blank, the absorbance of REP concentrations was measured spectrophotometrically at the estimated λ max of REP (242 nm) ***(Nasr-Eldin et al., 2024)***. A plot of a calibration curve was made. Three duplicates of the experiment were conducted.

Construction of calibration curve of REP in PBS pH 6.8 + 0.5% Tween 20

The smallest volume of phosphate buffered saline (PBS) pH 6.8 + 0.5% Tween 20 was used to dissolve 50 mg of (REP), and the volume was then raised to 1000 ml using PBS pH 6.8 + 0.5% Tween 20 (stock solution). Solutions containing 2.5, 5, 7.5, 10, 12.5, 15, 17.5, 20, 22.5, and 25 µg/ml were obtained by adding 10 ml of methanol to samples of 0.5, 1, 1.5, 2, 2.5, 3, 3.5, 4, 4.5, and 5 ml. Using PBS pH 6.8 + 0.5% Tween 20 as a blank, the absorbance of REP concentrations was measured spectrophotometrically at the estimated λ_{max} of REP (242 nm). A plot of a calibration curve was made. The experiment was repeated in triplicate ***(Nasr-Eldin et al., 2024)***.

Fabrication of Repaglinide loaded protransfersomes

Protransfersomal gel (PTG) was prepared with slight modifications as reported by Perrett et al ***(Chauhan and Gulati, 2016; Perrett et al., 1991)***. Briefly, 450 mg of Phospholipids, 90 mg of surfactant, Repaglinide (20mg) and ethyl alcohol were weighed and collected in an amber colored vial. All the components were mixed well in a clean, dry, wide mouth tube, with the help of a magnetic stirrer at a temperature of 60-70ºC, while keeping the open end of the vial closed, to prevent the loss of solvent. Then 100 µL phosphate buffer saline (pH 7.4) was added at the same temperature with continuous stirring, which lead to the formation of less viscous translucent liquid. The formed lipid vesicles were allowed to swell for 2 h at room temperature 25 °C. The multilamellar lipid vesicles (MLVs) were then sonicated for 2 min using a probe sonicator (ultrasonic processor, GE130, probe CV18, USA), the sonication cycle was carried out at 70% amplitude and Pulse of 10 seconds off and 50 seconds in an ice jacket to maintain the sonication temperature at 4 °C. then the dispersion was refrigerated until further characterization. This formula upon cooling was transformed to drug loaded protransfersomes which were stored under refrigeration (2–8 ◦C) ***(Gyanewali et al., 2021)***. Using the same procedure, different formulations containing different types of surfactants. The prepared protransfersome formulation was optimized based on particle size, PDI, and entrapment efficiency, The composition of formulations was shown **Tables (1-3)**.

Table (1): Composition of PTG using different edge activator

Formulation Code	EA*	PC: S*	Solvent used
F1	(Tween 80)	5:1	Ethanol
F2	(Span 60)	5:1	Ethanol
F3	(Polox 188)	5:1	Ethanol

Where, PC- Phosphatidyl choline (Soya Lecithin); S or EA- Surfactant or Edge activator

Table (2): Composition of PTG using different combination of edge activator.

Formulation Code	PC: S mix. *	S mix ratio	Surfactant	Solvent used
F4	5:1	1:1	(T80+Span 60)	Ethanol
F5	5:1	1:1	(T80+Polox. 188)	Ethanol
F6	5:1	1:1	(Span60+Polox. 188)	Ethanol

Where, PC- Phosphatidyl choline (Soya Lecithin); S mix- Surfactant mixture

Table (3): Formulation of REP loaded protransferosomes nanovesicles using different types of surfactants and combination of surfactant (edge activators)

Formulation Code	Amount of PC	Amount of surfactant	Surfactant	Solvent used
F1	450 mg	90 mg	(Tween 80)	Ethyl Alcohol
F2	450 mg	90 mg	(Span60)	Ethyl Alcohol
F3	450 mg	90 mg	(Polox. 188)	Ethyl Alcohol
F4	450 mg	90 mg (1:1)	(T.80+Span 60)	Ethyl Alcohol
F5	450 mg	90 mg (1:1)	(T.80+Polox.188)	Ethyl Alcohol
F6	450 mg	90 mg (1:1)	(Span 60+Polox. 188)	Ethyl Alcohol

Physicochemical characterization of REP-PTFs

Physical appearance:

Physical appearance: The gel was seen visually without the aid of any instruments to assess its color and physical state. The crystal properties of the Protransfersome gel were seen using an optical microscope at a magnification of 40X. This was done by spreading a small layer of the gel on a slide and placing a cover slip on top of it ***(Gupta et al., 2011b)***.

Particle size, polydispersity index and zeta potential analysis

The size and dispersion of vesicles were assessed by examining the transfersome dispersion, which consisted of hydrated protransfersome gel. The size of the transfersome vesicles was determined using the diffraction light scattering technique (DLS), namely the Malvern Zeta Sizer. The protransfersome was hydrated with phosphate buffer saline while being gently stirred, as described by ***(Jain et al., 2005)***. The REP-PTF formulation's particle size (PS), PDI, and zeta potential (ZP) were measured using the Malvern Zetasizer (Nano ZS; Malvern Instruments, Malvern, UK) at room temperature. The particle size was determined using the photon correlation spectroscopic (PCS) technique, while the ZP was measured using the electrophoretic light scattering technique ***(Rahman et al., 2023)***

Encapsulation efficiency % (EE)

The encapsulation efficiency %(EE) is the quantitative measure of the proportion of REP encapsulated within nanovesicles relative to the total amount of REP present in the nanovesicles dispersion. The encapsulation effectiveness of REP in protransfersome nanovesicles was assessed using an indirect method using high-speed cooling centrifugation (Beckman Instruments TLX-120 Optima Ultracentrifuge) centrifuged at 80000 rpm for 30 minutes at 4 °C. A total of 20 milligrams of

protransfersome were mixed with 10 milliliters of PBS (pH 6.8), then, 2 milliliters of the mixture were transferred to Eppendorf tubes and stored in a refrigerator at -20 °C. Afterward, the tubes were subjected to ultracentrifugation at a speed of 80000 rpm for 30 minutes at 4 °C. The dispersions were subjected to centrifugation to get the supernatant, which was then diluted with methanol in a 10 ml flask. The diluted solution was then analyzed using spectrophotometry at a wavelength of 242 nm ***(El-Sonbaty et al., 2022)***. The proportion of the drug that was successfully entrapped was determined using the following equations:

$$\% \text{ EE} = \frac{\text{Weight of initial drug} - \text{Weight of free drug}}{\text{Weight of initial drug}} \times 100$$

Particle morphology

The Protransfersome gel was hydrated with phosphate buffer saline (pH 6.8) while being gently agitated to form transfersome vesicles, which have certain shapes and surface features. Formulation morphology of REP-PTFs vesicles was observed visually via transmission electron microscope (TEM) (JEOL, JEM-1230, Tokyo, Japan) at 80 kilovolts (KV). Initially, samples of REP- PTFs were diluted with 1:200 double-distilled water and carried on a carbon-coated copper grid, and the samples were allowed to dry at room temperature overnight. The film on the grid was negatively stained by the addition of 2% uranyl acetate and left to dry at room temperature ***(El-Sonbaty et al., 2022; Nasr-Eldin et al., 2024)***. Then, the prepared samples were examined under TEM.

Drug-excipients compatibility studies

Fourier transform infrared spectroscopy (FT-IR)

For identification of the presence of any interaction between REP and the other ingredients of the REP-PTF (Repaglinide protransferosome), a FT-IR investigation was performed for pure Repaglinide, phospholipid, physical mixture of REP-PTFs components (1:1:1), blank, REP-PTF in addition to the surfactant used. Each sample to be measured is scanned in the wave number range of 4000~500 cm^{-1}). Briefly, KBr (spectroscopic grade) is placed in an oven for about 2 h at 105 $^{\circ}$C to eliminate the moisture. Each sample was mixed with dried KBr in 1:100, put in 13 mm die, and later compressed into pellets, using suitable pressure (usually 8 tons). An empty KBr disc is used as a blank to perform a background scan. The average of characteristic peaks of IR transmission spectra were recorded from triplicate samples ***(Li et al., 2021)***.

Differential Scanning Calorimetry (DSC) Studies

The thermal behavior of the bulk excipients and the degree of crystallinity and polymorphism of PTF formulations were analyzed using differential scanning calorimetry (DSC). Differential scanning calorimetry was used to acquire DSC thermograms of specific materials. The chosen samples underwent lyophilization in order to investigate the physical state and polymorphism of the REP-PTF. The DSC measurements were conducted with a Shimadzu DSC-50 (Japan), which is a differential

scanning calorimeter. The experiment involved placing pure REP, phospholipid, physical mixture, poloxamer 188, lyophilized blank of PTF, and lyophilized powder of REP-PTF in sealed aluminum pans. These pans were then heated at a temperature range of 25 °C to 250 °C, with a heating rate of 5 °C/min, until the powder reached a minimum amount of 3 mg. The nitrogen purge gas was consistently maintained at a flow rate of 30 mL/min. The reported data includes the melting point, enthalpies, and onset temperature of the observed transition ***(Nasr-Eldin et al., 2024; Yu et al., 2023)***. The heat flow amount was measured as a function of the sample temperature to investigate the thermal characteristics of nanoparticles.

In vivo evaluation studies (Pharmacodynamic effect)

To evaluate anti diabetic activity, adult male Sprague-Dawley rats (~250 g) were fasted overnight prior to the experiment. Diabetes mellitus was induced in rats by single intraperitoneal injection (120 mg/kg) of freshly prepared solution of alloxan monohydrate in normal saline ***(Tiss and Hamden, 2022)***. The animals were allowed to drink 5% glucose solution overnight to overcome the drug induced hypoglycemia. On the third day of injection, rats with blood glucose levels higher than 250 mg/ dl were considered diabetic and separated for the next day study. In order to confirm induction of diabetes mellitus in rats without complete destruction of β cells of Langerhans (mild alloxan induced diabetes mellitus), one rat was killed by decapitation under isoflurane anesthesia and tissue specimens from pancreas were fixed in 10% formalin solution for 24 h. Sections of 5 mm were stained with hematoxylin/eosin and photomicrographed using binocular microscope (Leica, Germany) ***(Alshora et al., 2023)***.

Hypoglycemic activity in rats, the rat's abdomen side hairs was removed by hair remover cream (Anne French) and wiped with diluted isopropyl alcohol on the previous day of the experiment. The rats were kept under observation for one week to allow the glucose level to stabilize, which has shown a rise due to fixation. The animals were divided into 5 groups (n = 6) group I considered as Negative control of (healthy normal) rats, and group II considered as Positive control (diabetic rats). The rats were treated as follows, Group-III – oral administration of 4 mg REP suspension (0.5% CMC), Group-IV – administrated plain REP suspended (3%CMC) patch, Group-V– administrated transdermal patch of REP-PTFs gel. All doses REP equivalent to 2 mg/kg ***(Sharma et al., 2015)***. Blood samples were collected from Retro Orbital- Sinuses of rats at different time intervals up to 24 h, (0, 0.25, 0.5, 1, 2, 4, 6, 8, 10, 12 and 24 h. after the treatment and blood glucose level was determined by using one touch glucodoctor. The hypoglycemic activity was determined as the percentage of reduction in blood glucose level and plotted against time.

Percent reduction in blood glucose level =

$$\frac{\textbf{Blood glucose at t} = \textbf{0 (starting time)} - \textbf{Blood glucose at t} = \textbf{t(0.25:24h)}}{\textbf{Blood glucose at t} = \textbf{0(starting time)}} \times \mathbf{100}$$

RESULTS and DISCUSSION

Analytical method development for Repaglinide:

UV scanning of Repaglinide

The UV scan of REP exhibited absorption peaks at 242 nm in absolute methanol, which aligns with the λ_{max} of Repaglinide reported in scientific literature ***(Nasr-Eldin et al., 2024)***, as depicted in **Figure (1)**

Construction of calibration curve of REP in methanol

Figure (2A) shows the absorbance of REP after serial dilution (2.5–25 µg/ml) in methanol, which showed a linear relationship (R = 0.9992) between the absorbance obtained and REP concentrations, which indicated that the REP obeys Beer-Lambert´s law λ_{max} (242 nm).

Construction of calibration curve of REP in PBS (pH 6.8) + 0.5 % Tween 20

Figure (2B) showed the absorbance of REP after serial dilution (2.5 -25 µg/ml) in PBS pH 6.8 + 0.5% Tween 20 while, which showed a linear relationship (R=0.9992) between the absorbance obtained and REP concentrations which indicated that, the REP obeys Beer-Lambert law at λ_{max} (242 nm).

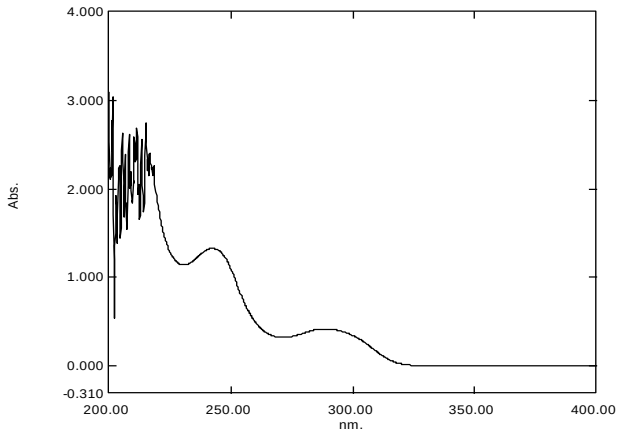

Figure (1): UV Scanning of Repaglinide in methanol

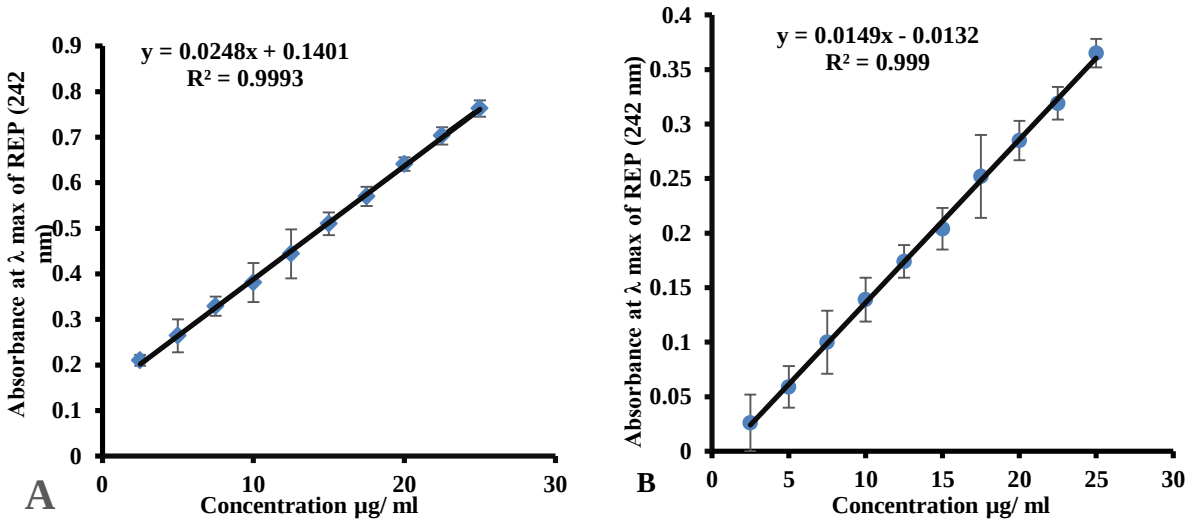

Figure (2): Standard calibration curve for REP in (A) methanol and (B) Phosphate buffer Ph 6.8 + 5% Tween 20 at λ_{max} of (242 nm)

Fabrication of Repaglinide protransfersomes (REP-PTF)

A successful attempt was made to formulate Repaglinide loaded on protransferosomes gel using different surfactants. The effect of different types of surfactants applied on formulations was assessed. In the present work, six formulations were prepared, and composition is mentioned in **Table (4)** Among these one of the best formulations was chosen for further investigation. The prepared Repaglinide Protransfersome formulation was aimed for transdermal application. Thus, vesicle size and vesicle size distribution of protransfersomes are crucial parameters for transdermal permeation of such formulation. The effect of surfactant and phospholipids have an immense effect on vesicle size and distribution. All batches showed a small mean size, well suited for transdermal permeation. The mean particle size by diffraction light scattering lies between 184 - 629 nm ranges. The composition of formulations is shown in **Table (4).**

Table (4): Suggested formulae of REP loaded protransferosomes nanovesicles using different types of surfactants and combination of surfactant (edge activator)

FN	Drug	Amount of PC	Amount of surfactant	Surfactant EA	Solvent
F1	20 mg	450 mg	90 mg	(Tween 80)	Ethyl Alcohol
F2	20 mg	450 mg	90 mg	(Span60)	Ethyl Alcohol
F3	20 mg	450 mg	90 mg	(Polox 188)	Ethyl Alcohol
F4	20 mg	450 mg	90 mg (1:1)	(T80+Span60)	Ethyl Alcohol
F5	20 mg	450 mg	90 mg (1:1)	(T80+Polox188)	Ethyl Alcohol
F6	20 mg	450 mg	90 mg (1:1)	(Span60+Polox188)	Ethyl Alcohol

Table (5): Particle size, polydispersity indices, zeta potential and entrapment efficiency of REP-PTFs formulations.

F. N	PS (nm)	PDI	ZP (mV)	EE (%)
F1	184.7± 9.7	0.627±0.041	−29.1±1.03	85.3±2.2
F2	602.1± 20.9	0.491±0.045	−31.5±0.95	80.9±6.5
F3	629.7 ± 172.5	0.804±0.173	−32.5±1.81	92.8±5.8
F4	319.5± 16.9	0.764±0.164	−33.87±1.64	78±4.9
F5	296.8 ±40.3	0.465±0.072	−35.05±2.6	95.8±3.2
F6	545.6±77.3	0.627±0.094	−37.77±1.77	93.7±2.9

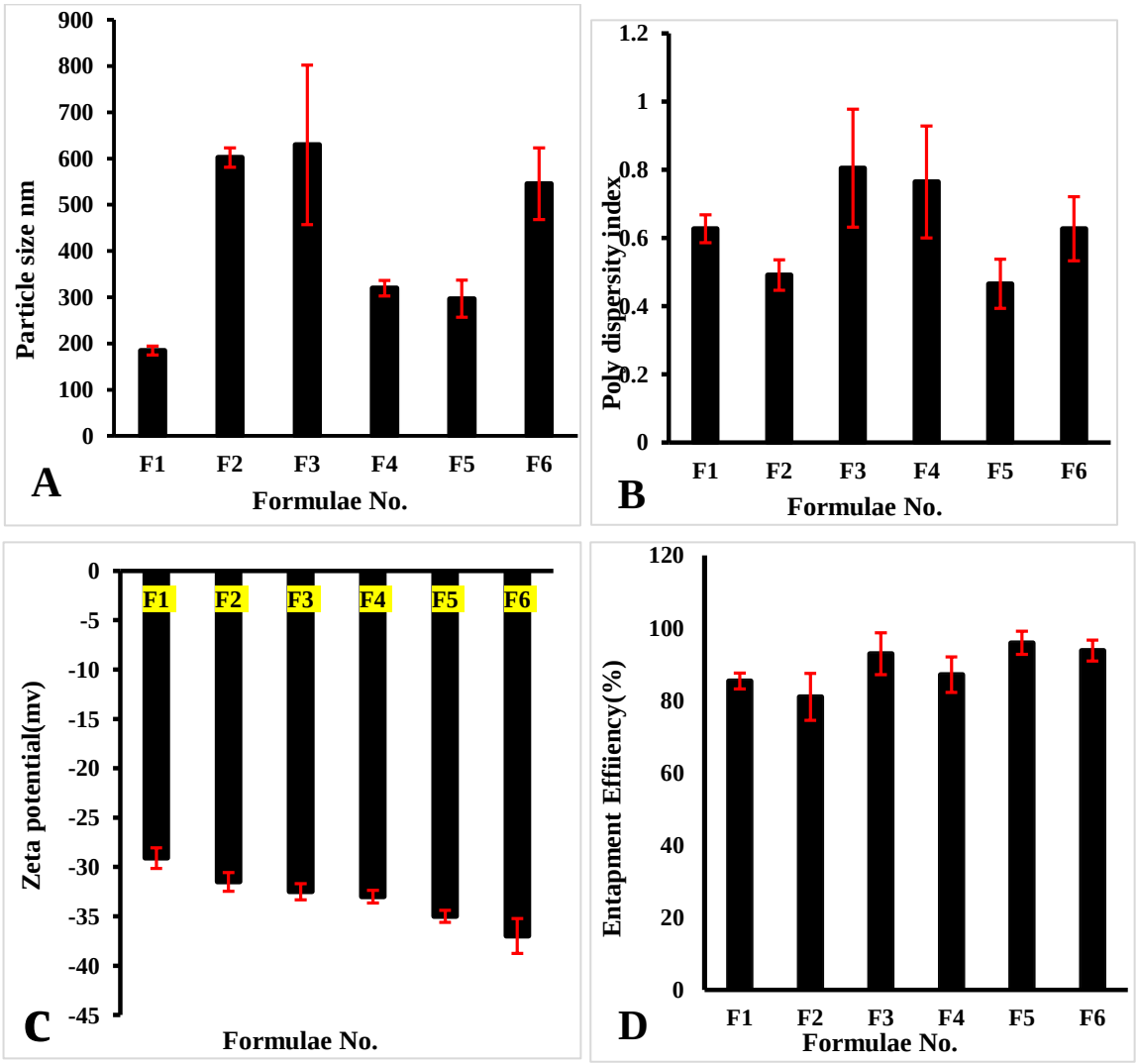

Figure (3): Histogram showing (A) the mean PS, (B) PDI, (C) ZP and (D) %EE of REP-PTFs formulations

Physicochemical Characterization of (REP-PTFs)

Physical appearance

The prepared Protransfersome formulations were viewed by naked eye to characterize color and physical state of gel. The results of physical appearance are yellowish semisolid compact mass. The prepared Repaglinide Protransfersome formulation was aimed for transdermal application. Thus, vesicle size and vesicle size distribution of protransfersomes are crucial parameters for transdermal permeation of such formulation.

Particle size

The particle size of six formulations lies between 184.7 – 629.7 nm which is a convenient nano-range. A recent study shows that lipid-based vesicles with particle sizes between 100 and 600 nm are better at getting into the skin than those with larger particle sizes, in particular protransfersomes (PTF) ≤ 300 nm gets deeper into the skin ***(Demartis et al., 2021).*** From the results reported in **Table (5)** and depicted in **Figure (3A)**, it was found that REP-PTFs prepared with Tween 80 have a smaller vesicle size (184.7 ± 9.7) nm than those prepared with Span 60 (602.1 ± 20.9). This may be attributed to the general concept of the use of surfactant with a higher HLB which resulted in the preparation of vesicles with smaller sizes ***(Singh et al., 2016)***. Tween 80 is water-soluble surfactant with a HLB value of 15 and therefore the presence of a water-soluble surfactant in protransfersomes enabled lower vesicle size, when compared to the employment of Span 60, which are oil soluble and water dispersible surfactants (i. e. HLB values of 4.3 and 8.6). It is suggested that the hydrophilic surfactant (Tween 80) covers the surface of the vesicles more due to their hydrophilic moiety (higher HLB value, when compared to Span 60. These results are in agreement with studies conducted by previous researchers ***(Bnyan et al., 2019)***.

The optimal Hydrophilic Lipophilic Balance (HLB) value for producing a stable Oil-in-Water (O/W) emulsion is typically within the range of 12 to 16, as suggested by ***(Abd El-Halim et al., 2020; Chen et al., 2014)***. This might be the reason for larger Protransfersome prepared using Pluronic® F68 as a single surfactant (629.7±172.5) where Pluronic® F68 has HLB value larger than 24 ***(Das et al., 2012)***. Moreover, the hydrophilicity of the surfactant head group also contributes to reducing the size of the vesicles, which could be linked to the smaller hydrophobic core. The findings align with study completed by prior scholars ***(Bnyan et al., 2019)***. Finally, combination of surfactant leads to the presence of enough surfactant to coat and stabilize the fine droplets of the lipids and hinder the coalescence of the nano-sized globules as in (F4, F5 and F6). This might be attributed to the resulted reduction in the interfacial tension of the phospholipid droplets leading to the disruption of the phospholipid droplets into smaller ones (319.5 ± 16.9) nm, (296.8 ± 40.3) nm and (545.6 ± 77.3) nm respectively.

Polydispersity index

PDI is employed to assess the average uniformity of particle size. Higher PDI values suggest a greater degree of variation in the size distribution of the particle

sample. The acceptable range for PDI lies between 0.08 to 0.7. A summary of the data obtained from measuring PDI as reported in **Table (5)** and depicted in **Figure (3B)**. REP-PTFs were prepared had a PDI value of < 0.804 ± 0.173, which was obtained via the chosen preparation process. This result indicates that the nanoparticles in the REP-PTFs have a uniform and narrow size distribution. Furthermore, this PDI value falls within the allowed range of 0.08-0.7 for PDI except F3. The same rationale has been documented by ***(Clayton et al., 2016)***.

Zeta potential measurement

The Zeta potential values for all the formulated designs are reported in **Table (5)** and depicted in **Figure (3C)**. The results indicated that the different formulations had a consistently negative surface charge, and this negative charge effectively prevented particle aggregation. This negative charge was ascribed to the anionic properties of the phospholipids or due to the presence of non-ionic surfactants, which often confer a negative charge to particles on which they are adsorbed ***(Abdou et al., 2017; Al-mahallawi et al., 2021)***. Also, the negative value of zeta potential derived from the nonionic surfactant are attributable to polarization of the surfactant, followed by adsorption of polarized water molecules at the surface of the PTF ***(Zhao et al., 2014)***. The ZP values of all formulations range from -37.77±1.77 to -29.1±1.03 mV. Additionally, Span and Tween 80 are a nonionic surfactant, so protransfersomes comprised of nonionic surfactant as an edge activator could have negatively charged surface due to the partial hydrolysis of polyethylene oxide head groups [i.e., (CH2-CH2-O) n] of the Span® 80 or Tween® 80 ***(Ahad et al., 2018)***. The nonionic surfactant utilized in this investigation exhibits superior steric stabilization and inferior electrostatic stabilization, resulting in the formation of a well-formed coating over the particles of REP-PTFs. Poloxamer 188 exerts steric stabilization, which inhibits the aggregation of nanoparticles inside the colloidal system ***(Wei and Ge, 2012)***. Thus, Poloxamer 188 is essential in determining the zeta potential and stability of REP-PTFs.

% Entrapment Efficiency

Types of surfactants were found to affect entrapment efficiency as illustrated in table in **Table (5)** and represented in **Figure (3D)**. The encapsulation efficiencies were found to vary between 80.9% and 95.8 %. The relatively high encapsulation efficiencies of REP in the prepared REP-PTFs might be due to the lipophilic properties of REP which enhance the solubility of REP in phospholipid lipids and subsequently improve the E.E. Chemical structure of phospholipids plays an important role in drug loading where phospholipids forming less ordered crystalline structure with many imperfections have a large void space in which REP can be entrapped leading to improvement in E.E. The high entrapment efficiency of REP in PTFs can be attributed to its high lipophilic nature (log p ~ 3.92), which improves the solubility of REP in phospholipids and allows for easy incorporation into the phospholipids ***(Soni et al., 2020)***. All formulations with poloxamer188 have good entrapment capacity in comparison to formulation with other single surfactant or in combination. Regarding types of surfactants, it was found that Protransfersome prepared using Tween® 80 (F1) have low E.E (85.3±2.2 %) from REP-PTFs prepared using Pluronic® F68 (F3) (92.8±5.8 %). Because Pluronic® F68 act as steric stabilizer through creating an effective coat on the surface of REP-PTFs

which subsequently prevents REP leakage to the external phase and thus retain high concentration of REP inside protransfersome ***(Abdelbary and Fahmy, 2009; Nasr-Eldin et al., 2024)***.

Additionally, it was found that REP-PTFs prepared with Tween 80 (F1) have a higher % EE (85.3±2.2 %) than those prepared with Span 60 (F2) (80.9±6.5 %). These results may be attributed to (HLB) values of these surfactants. The HLB values of Tween 80 and Span 60 were 15 and 4.7 respectively. Hence, lipophilic surfactants (Span 60) also compete with lipophilic molecules (i.e., REP) to assemble themselves in the bilayers, which may result in a larger vesicle size, but also leave less space for REP entrapment, providing an explanation for the low entrapment observed ***(Khan et al., 2021)***. Furthermore, it is also suggested that Span 60 contains an unsaturated double bond in their alkyl carbon chain, and therefore lower bilayer domain available to house REP (lipophilic drug molecule). Furthermore, the entrapment efficiency of formulations containing a combination of two surfactants as in (F4, F5, and F6) have higher entrapment efficiency than formulations containing a single surfactant (F1, F2 and F3) have low EE due to the synergistic effect of surfactants ***(Gupta et al., 2011a; Xinying et al., 2023)***.

Rank order for the different formulations of REP-PTFs

As appeared in **Table (6)** the rank order was performed for all prepared REP-PTFs formulations (F1 to F6) in order to choose the best formula based on the previous measured characterization as Particle size (PS), polydispersity index (PDI), zeta potential (ZP), and % encapsulation efficiency of REP-PTFs where in the formula (**F5**) which composed of surfactant (Poloxamer 188 + Tween 80) was chosen as the best formula for further investigations as depicted in **Figure (4A)** and **Figure (4B)** which showed the mean particle size and zeta potential respectively.

Table (6): Rank order of REP-PTFs formulations

F. N	Edge activators	PS	PDI	ZP	% EE	TOTAL	R. O
F1	A (T.80)	1	4	6	5	16	4
F2	B (Span 60)	5	2	5	6	18	5
F3	C (Polox. 188)	6	6	4	3	19	6
F4	D (T.80+Span 60)	3	5	3	4	15	3
F5	E (T.80+Polox.188)	2	1	2	1	6	1
F6	F (Span 60+Polox.188)	4	3	1	2	10	2

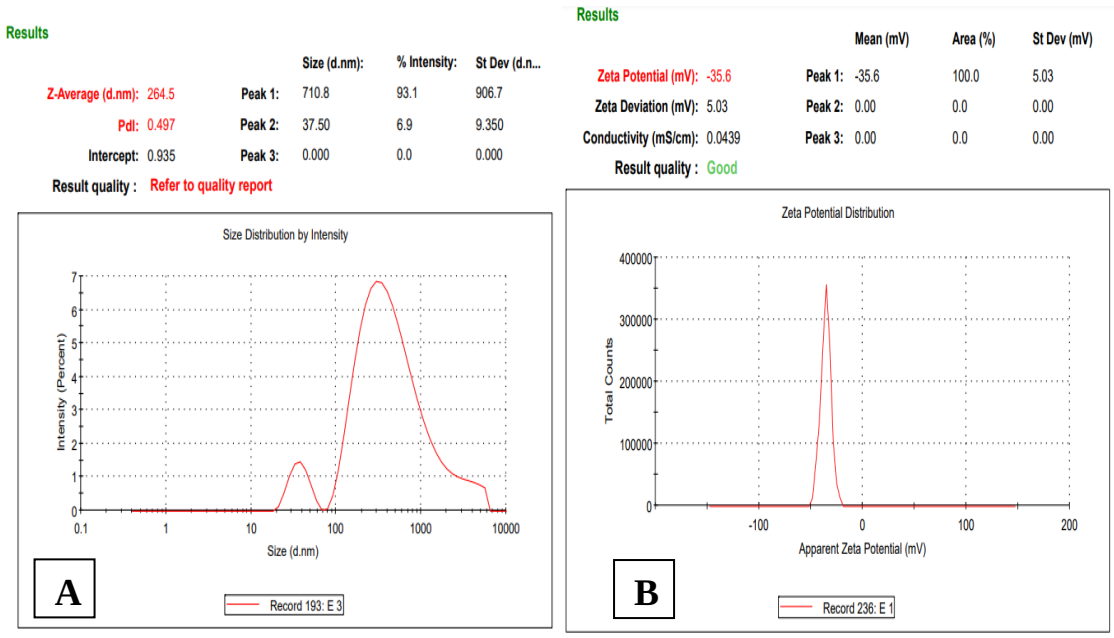

Figure (4): (A) Particle size of the best formulae (F5) taken from three charts and (B) Zeta potential of the best formulae (F5) taken from three charts.

Particle Morphology

The morphological appearance of protransfersome NVs containing Repaglinide (REP-PTFs) was visualized using a transmission electron microscope (TEM) with a magnification of 20,000 times. The image clearly demonstrates that the REP-PTFs vesicles exist as distinct entities. All particles depicted in the photograph were inside the nanometer scale. The transmission electron microscopy (TEM) analysis demonstrated that the nanovesicles in the REP-PTFs formulation exhibited a uniform ellipsoidal or spherical morphology, as depicted in **Figure (5)**.This might indicate homogeneity and good uniformity the The vesicles appear smaller when measured nanovesicles of REP-PTFs using TEM compared to DLS due to the drying process involved in preparing the TEM sample. This causes the nanoparticles to shrink, resulting in a smaller size compared to the diffraction light scattering DLS measurement. Where in DLS, the hydration of the samples maintains the size of the nanoparticles ***(Elkarray et al., 2022; Swidan et al., 2018)***.

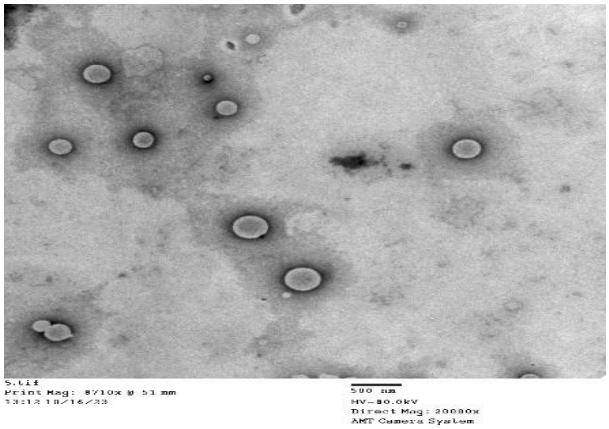

Figure (5): TEM image of the best selected REP-PTFs formula (F5)

Drug-excipients compatibility studies

Fourier transform infrared spectroscopy (FT-IR)

FT-IR is a technique used to investigate the structural characteristics of phospholipid and to assess the molecular interactions between a drug and the excipients used in formulations ***(Imran et al., 2022)***. The characteristic spectrum of REP, Phospholipid, Poloxamer 188, Blank PTFs and Optimum formula are shown in **Figure (6)**. The FTIR spectrum of REP exhibits peaks at 3307.73 cm^{-1} which corresponds to the stretching of the (NH) group. Additionally, there are peaks at 2934.6 cm^{-1} corresponding to (CH stretching), and bands at 1687.6 cm^{-1} representing C=O stretching in the carboxylic acid group ***(Nasr-Eldin et al., 2024)***. The bands at 1040.4 cm^{-1} and 1214 cm^{-1} are related to (C–O stretching) in phenyl alkyl ether structure. The bands at 1568.4 cm^{-1} and 1634.4 cm^{-1} are due to (aromatic C = C and N–H bending) respectively ***(Maddiboyina et al., 2021)***, Peaks at 1490.9 to 1449.3 cm^{-1} attributed to CH deformation, Additionally, the peak observed at 1215.1 cm^{-1} can be attributed to –CH3 stretching.

The characteristic bands of the Poloxamer 188 ranging from 964.3 cm^{-1} to 1115.01 cm^{-1}, can be attributed to the symmetrical structure of C–O and the asymmetric stretching vibrations of C–O in the ether groups of –OCH2CH2 residues that are present throughout the Poloxamer 188 structure. Additionally, the molecule exhibited −OH stretching vibrations at 2884.39 cm^{-1} and 1344.6 cm^{-1} (in-plane O–H bend). These findings are supported by previous studies conducted by ***(Elkarray et al., 2022)***. Tween 80 demonstrated peaks at 3434.97 cm^{-1} (O−H stretching), 2922 cm^{-1} (–CH2– asymmetric stretching), 2858 cm^{-1} (–CH2– symmetric stretching), and 1734.52 cm^{-1} (C=O stretching, ester group), and 1093 cm^{-1} (C–O stretching), ***(Abootorabi et al., 2022)***. Phospholipon G 90 (PG90) spectrum was shown strong sharp peaks of the characteristic C–H stretching bands at 2925 cm^{-1}, 2853 cm^{-1}. A stretching band of ester carbonyl group was observed at 1736 cm − 1, and an ester C–O stretching band also recorded at 1252 cm^{-1} ***(Elsheikh et al., 2023)***.

The PTFs blank exhibited several characteristic peaks with strong intensity of CH stretching at 2914.53 and 2849.95, and C=O stretching at 1737.81 cm^{-1} from carboxyl group, respectively, which are the typical bands of phospholipid. After the PTF was emulsified with the presence of poloxamer, the absorption bands at 2915 and 2849 cm^{-1} did not shift, but the intensity of both peaks were reduced and the absorption band at 1181.02 cm^{-1} disappeared. This may be explained by the increased hydrophilic nature and the shielding effect of the amphiphilic surfactant. Meanwhile, a new characteristic peak with strong intensity at 1100.66 cm^{-1} was observed as a result of strong stretching of C-O-C linkage from poloxamer 188 ***(Luo et al., 2015)***. While FTIR spectrum of the selected REP-PTFs formula showed some peaks such as N–H stretch of REP was covered by O–H stretch of phospholipid. The positions of the mentioned bands especially for those in phospholipid were changed indicating the presence of hydrogen bonding between REP and phospholipid as showed in **Figure (6)**. This finding interprets the achieved high drug encapsulation ***(Tupal et al., 2016)***.

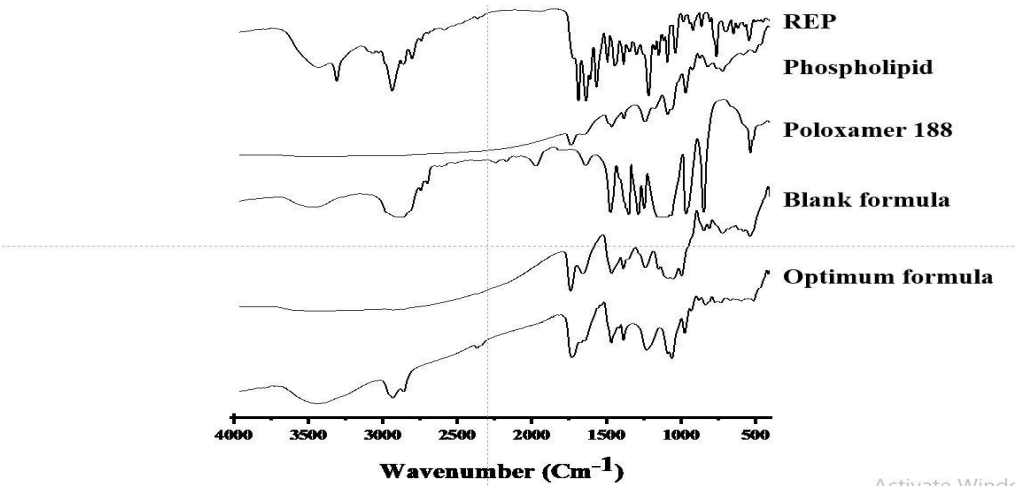

Figure (6): FTIR spectrum REP, Phospholipid, Poloxamer 188, Blank PTFs and Optimum formula (F5)

Differential scanning calorimetry (DSC)

The characterization of the crystallinity of PTFs is important because it can influence encapsulation and drug release. DSC studies were performed to obtain information about the crystallinity of the PTFs and the interactions between the drug and phospholipids in the formulation. Differential scanning colorimetry (DSC) is a precise, fast, and dependable method for determining the crystallinity of a drug. It also provides a good indication of the probable interactions between additives and drugs during formulation. These interactions can be expressed in thermograms through the appearance of new peaks, endothermic displacement peaks, or a change in the structure/peak enthalpy***(Sharma et al., 2023)***.

DSC analysis of pure Repaglinide

Pure REP showed a sharp endothermic peak at 138°C as showed in **Figure (7)**, which was consistent with its melting point and reflecting its crystalline structure. This

peak is in accordance with its standard that is stated in the literature ***(PATEL and KHAN, 2023)***. DSC analysis of the selected REP-PTFs, the typical endothermic peak of REP shifted, indicating its entrapment in the phospholipid matrix, and converted to amorphous state from crystalline state ***(Elkarray et al., 2022; Swidan et al., 2018)***. Shifting of endothermic peak of REP in the PTFs formulations confirms the conversion of crystalline state to molecularly dispersed amorphous state within the nanoparticle formulations as showed in **Figure (7)**. These findings are also in agreement with the very high EE.

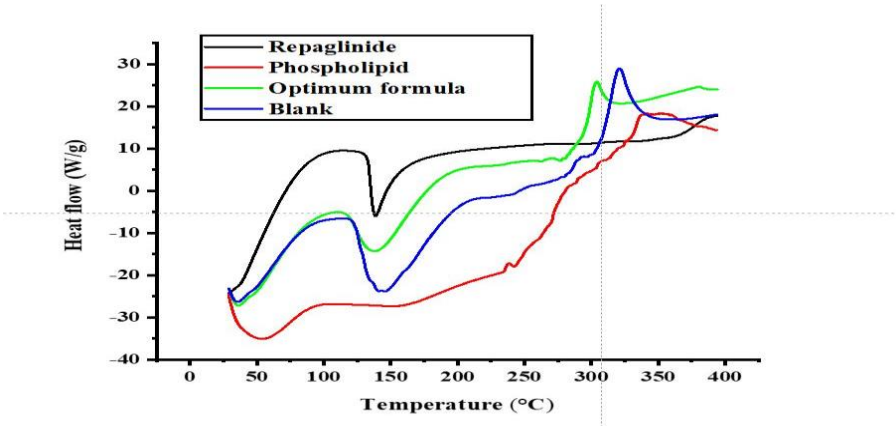

Figure (7): DSC analysis of REP, Phospholipid, Blank PTFs and Optimum formula

In vivo evaluation studies (Pharmacodynamic effect)

Alloxan is a cytotoxic compound that is similar to glucose and is used to induce diabetes mellitus in animals. It achieves this by destroying the β cells of Langerhans, which leads to a decrease in insulin production and release ***(Tiss and Hamden, 2022)***. On the other hand REP induces a hypoglycemic effect by stimulating the secretion of insulin from pancreatic β cells, consequently REP is effective in treating moderate diabetes caused by alloxan, but ineffective in treating severe alloxan-induced diabetes ***(Elbahwy et al., 2017; Nasr-Eldin et al., 2024)***. A histological examination was conducted to verify the establishment of moderate diabetes in the rat Figure **(8A)** displays histological photomicrographs of pancreas specimens. The pancreas tissue samples from the control rats exhibited normal structure, with intact islets of Langerhans and acini cells. However, the samples from the diabetic rats showed pancreatic islets with areas of fibrosis, vacuolation, and some cells displaying pyknosis, indicating a partial loss of beta cells as shown in **Figure (8B)**.The results confirmed the induction of moderate diabetic mellitus in rats with the use of alloxan induction ***(Bacevic et al., 2020)***.

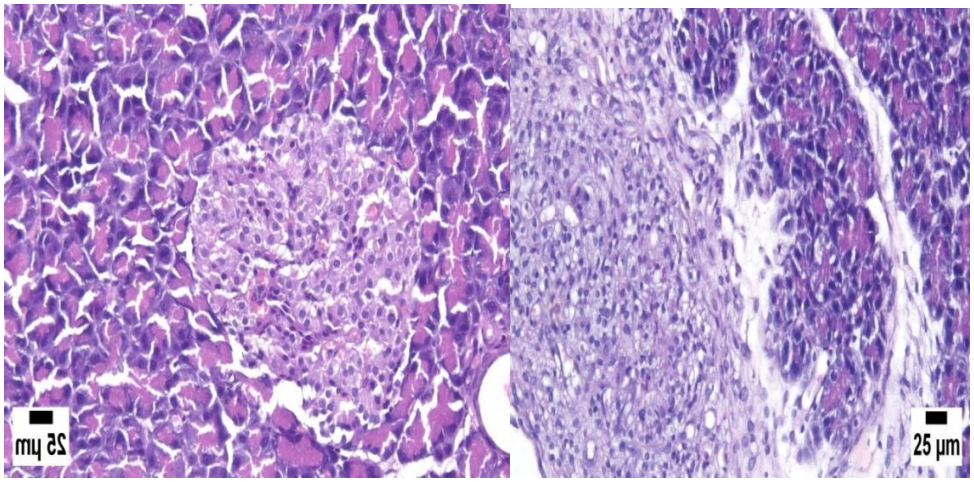

A **B**

Figure (8): Photomicrograph of pancreas (A) Normal control group showing normal histology of normal islets of Langerhans exocrine acini (H&E) and (B) Diabetic control group numerous inflammatory cells infiltration in the peripancreatic tissue (arrow (H&E)

The effectiveness of the developed REP-PTF-NVs formulation in improving the anti-glycaemic effect of REP was investigated in-vivo on male rats rendered diabetic by single intraperitoneal injection (120 mg/kg) of freshly prepared solution of alloxan monohydrate in normal saline ***(Tiss and Hamden, 2022)*** in comparison with the simple aqueous dispersion of the drug, both orally administered by gavage (2 mg kg^{-1} body weight) ***(Sharma et al., 2015)*** and transdermal patch of pure REP suspensded (3 % CMC) GEL in both normal and diabetes rats. The results, collected in **Table (7)** and represented in **Figure (9)**.

All animals were administered single dose of REP equivalent to 2 mg/kg ***(Sharma et al., 2015)*** Group I administrated plain REP suspension (0.5% CMC) oral, and group II received plain REP suspended (3 % CMC) gel by transdermal routes, and group III received REP-PTFs gel by transdermal routes. The result has shown reduction in plasma glucose levels in transdermal patch containing REP-PTFs in comparison with oral and transdermal administration of Repaglinide (2 mg) in diabetes rats. The observed hypoglycemic effect was found to be significant in case of REP-PTFs transdermal patch treated animals ($P < 0.001$), when compared to orally treated animals up to 24 h. The Repaglinide (oral) produced a decrease in blood glucose level for 4 h. In the case of transdermal patches containing nanoparticles (2 mg), the hypoglycemic response was gradual. A maximum hypoglycemic response was observed after 24h and remained stable in REP-PTF.

Table (7): Effect of REP OS, REP-TG and REP-PTF gel on blood glucose level of diabetic rat

Time hours	Group I		Group II		Group III		Group IV		Group V	
	Negative control		Positive control (Diabetic)		Oral (REP)		Transdermal REP gel		REP-PTFs gel	
	Average	±SD	average	±SD	average	±SD	Average	±SD	Average	±SD
0	89	2.4	491	82.5	560	77	574	94.6	520	114
0.15	93	5.7	511	88.4	576	89	595	138.9	498	91.4
0.30	87	8.6	530	118.8	570	100.5	561	77.8	510	111.8
1	88	6.7	536	111.8	436	95.4	490	67.4	470	74.4
2	92	8.9	525	77.4	381	43.9	454	71.4	413	56.6
4	90	7.4	520	91.1	310	61.2	417	44.7	423	67.9
6	88	9.8	529	102.2	270	37.5	306	50.8	375	27.9
8	85	9.3	495	50.5	350	66.9	340	58.8	250	32.1
10	80	10.7	510	59.3	380	58.4	233	42.4	216	26.1
12	85	4.3	615	80.4	430	99.7	415	60.5	190	14.8
24	82	5.8	485	76.8	640	119.9	564	39.6	132	17.7

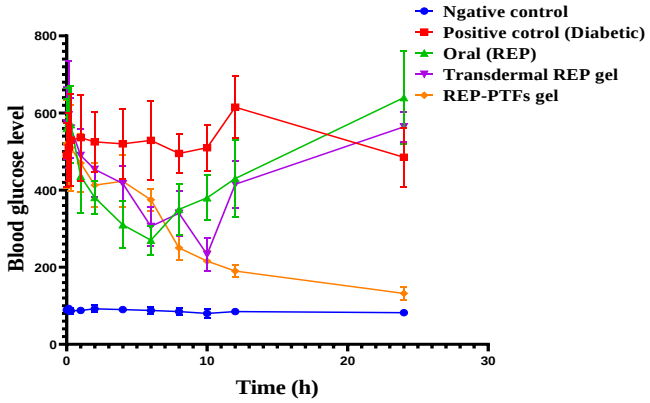

Figure (9): Effect of REP OS, REP-TG and REP-PTF gel (F5) on blood glucose level of diabetic rat

REFERENCES

Abd El-Halim, S.M., Abdelbary, G.A., Amin, M.M., Zakaria, M.Y., Shamsel-Din, H.A., and Ibrahim, A.B. (2020). Stabilized oral nanostructured lipid carriers of Adefovir Dipivoxil as a potential liver targeting: Estimation of liver function panel and uptake following intravenous injection of radioiodinated indicator. DARU Journal of Pharmaceutical Sciences *28*, 517-532.

Abdelbary, G., and Fahmy, R.H. (2009). Diazepam-loaded solid lipid nanoparticles: design and characterization. Aaps Pharmscitech *10*, 211-219.

Abdou, E.M., Kandil, S.M., and El Miniawy, H.M. (2017). Brain targeting efficiency of antimigrain drug loaded mucoadhesive intranasal nanoemulsion. International journal of pharmaceutics *529*, 667-677.

Ahad, A., Al-Saleh, A.A., Al-Mohizea, A.M., Al-Jenoobi, F.I., Raish, M., Yassin, A.E.B., and Alam, M.A. (2018). Formulation and characterization of Phospholipon 90 G and tween 80 based transfersomes for transdermal delivery of eprosartan mesylate. Pharmaceutical development and technology *23*, 787-793.

Al-mahallawi, A.M., Ahmed, D., Hassan, M., and El-Setouhy, D.A. (2021). Enhanced ocular delivery of clotrimazole via loading into mucoadhesive microemulsion system: In vitro characterization and in vivo assessment. Journal of Drug Delivery Science and Technology *64*, 102561.

Alshora, D., Ibrahim, M., Alanazi, N., Alowyid, M., Alnakhli, Z.A., Alshiban, N.M., Maodaa, S., Alyami, N.M., and Alotaibi, I. (2023). Formulation of Glibenclamide proniosomes for oral administration: Pharmaceutical and pharmacodynamics evaluation. Saudi Pharmaceutical Journal *31*, 101830.

Bacevic, M., Rompen, E., Radermecker, R., Drion, P., and Lambert, F. (2020). Practical considerations for reducing mortality rates in alloxan-induced diabetic rabbits. Heliyon *6*.

Bnyan, R., Khan, I., Ehtezazi, T., Saleem, I., Gordon, S., O'Neill, F., and Roberts, M. (2019). Formulation and optimisation of novel transfersomes for sustained release of local anaesthetic. Journal of Pharmacy and Pharmacology *71*, 1508-1519.

Chauhan, M.K., and Gulati, A. (2016). Aggrandized transdermal delivery of glimepiride via transfersomes: formulation, evaluation and statistical optimisation. Journal of Drug Delivery and Therapeutics *6*, 48-54.

Chen, Y., Yang, X., Zhao, L., Almásy, L., Garamus, V.M., Willumeit, R., and Zou, A. (2014). Preparation and characterization of a nanostructured lipid carrier for a poorly soluble drug. Colloids and surfaces A: physicochemical and engineering aspects *455*, 36-43.

Clayton, K.N., Salameh, J.W., Wereley, S.T., and Kinzer-Ursem, T.L. (2016). Physical characterization of nanoparticle size and surface modification using particle scattering diffusometry. Biomicrofluidics *10*.

Das, S., Ng, W.K., and Tan, R.B. (2012). Are nanostructured lipid carriers (NLCs) better than solid lipid nanoparticles (SLNs): development, characterizations and comparative evaluations of clotrimazole-loaded SLNs and NLCs? European journal of pharmaceutical sciences *47*, 139-151.

Demartis, S., Rassu, G., Murgia, S., Casula, L., Giunchedi, P., and Gavini, E. (2021). Improving dermal delivery of rose bengal by deformable lipid nanovesicles for topical treatment of melanoma. Molecular Pharmaceutics *18*, 4046-4057.

Ebrahimi, H.A., Javadzadeh, Y., Hamidi, M., and Jalali, M.B. (2015). Repaglinide-loaded solid lipid nanoparticles: effect of using different surfactants/stabilizers on physicochemical properties of nanoparticles. DARU Journal of Pharmaceutical Sciences *23*, 1-11.

El-Sonbaty, M.M., Akl, M.A., Khalid, M., and Kassem, A.A. (2022). Does the technical methodology influence the quality attributes and the potential of skin permeation of Luliconazole loaded transethosomes? Journal of Drug Delivery Science and Technology *68*, 103096.

Elbahwy, I.A., Ibrahim, H.M., Ismael, H.R., and Kasem, A.A. (2017). Enhancing bioavailability and controlling the release of glibenclamide from optimized solid lipid nanoparticles. Journal of drug delivery science and technology *38*, 78-89.

Elkarray, S.M., Farid, R.M., Abd-Alhaseeb, M.M., Omran, G.A., and Habib, D.A. (2022). Intranasal repaglinide-solid lipid nanoparticles integrated in situ gel outperform conventional oral route in hypoglycemic activity. Journal of Drug Delivery Science and Technology *68*, 103086.

Elsheikh, M.A., Gaafar, P.M., Khattab, M.A., Helwah, M.K.A., Noureldin, M.H., and Abbas, H. (2023). Dual-effects of caffeinated hyalurosomes as a nano-cosmeceutical gel counteracting UV-induced skin ageing. International Journal of Pharmaceutics: X *5*, 100170.

Gamsjaeger, S., Fratzl, P., and Paschalis, E. (2021). Interplay between mineral crystallinity and mineral accumulation in health and postmenopausal osteoporosis. Acta Biomaterialia *124*, 374-381.

Gupta, M., Vaidya, B., Mishra, N., and Vyas, S.P. (2011a). Effect of surfactants on the characteristics of fluconazole niosomes for enhanced cutaneous delivery. Artificial Cells, Blood Substitutes, and Biotechnology *39*, 376-384.

Gupta, V., Agrawal, R.C., and Trivedi, P. (2011b). Reduction in cisplatin genotoxicity (micronucleus formation) in non target cells of mice by protransfersome gel formulation used for management of cutaneous squamous cell carcinoma. Acta Pharm *61*, 63-71.

Gyanewali, S., Kesharwani, P., Sheikh, A., Ahmad, F.J., Trivedi, R., and Talegaonkar, S. (2021). Formulation development and in vitro–in vivo assessment of protransfersomal gel of anti-resorptive drug in osteoporosis treatment. International Journal of Pharmaceutics *608*, 121060.

Imran, B., ud Din, F., Ali, Z., Fatima, A., Khan, M.W., Kim, D.W., Malik, M., Sohail, S., Batool, S., and Jawad, M. (2022). Statistically designed dexibuprofen loaded solid lipid nanoparticles for enhanced oral bioavailability. Journal of Drug Delivery Science and Technology *77*, 103904.

Ita, K. (2014). Transdermal drug delivery: Progress and challenges. Journal of Drug Delivery Science and Technology *24*, 245-250.

Jain, S., Sapre, R., Tiwary, A.K., and Jain, N.K. (2005). Proultraflexible lipid vesicles for effective transdermal delivery of levonorgestrel: development, characterization, and performance evaluation. Aaps Pharmscitech *6*, E513-E522.

Kesharwani, R., Patel, D.K., and Yadav, P.K. (2022). Bioavailability enhancement of repaglinide using nano lipid carrier: Preparation characterization and in vivo evaluation. Int. J. Appl. Pharm. *14*, 181-189.

Khan, I., Needham, R., Yousaf, S., Houacine, C., Islam, Y., Bnyan, R., Sadozai, S.K., Elrayess, M.A., and Elhissi, A. (2021). Impact of phospholipids, surfactants and cholesterol selection on the performance of transfersomes vesicles using medical nebulizers for pulmonary drug delivery. Journal of Drug Delivery Science and Technology *66*, 102822.

Khatoon, K., Rizwanullah, M., Amin, S., Mir, S.R., and Akhter, S. (2019). Cilnidipine loaded transfersomes for transdermal application: formulation optimization, in-vitro and in-vivo study. Journal of Drug Delivery Science and Technology *54*, 101303.

Li, N., Li, X., Cheng, P., Yang, P., Shi, P., Kong, L., and Liu, H. (2021). Preparation of Curcumin Solid Lipid Nanoparticles Loaded with Flower-Shaped Lactose for Lung Inhalation and Preliminary Evaluation of Cytotoxicity In Vitro. Evidence-Based Complementary and Alternative Medicine *2021*, 1-15.

Luo, Y., Teng, Z., Li, Y., and Wang, Q. (2015). Solid lipid nanoparticles for oral drug delivery: chitosan coating improves stability, controlled delivery, mucoadhesion and cellular uptake. Carbohydrate polymers *122*, 221-229.

Maddiboyina, B., Jhawat, V., Nakkala, R.K., Desu, P.K., and Gandhi, S. (2021). Design expert assisted formulation, characterization and optimization of microemulsion based solid lipid nanoparticles of repaglinide. Progress in Biomaterials *10*, 309-320.

Nasr-Eldin, M.A., Elbahwy, I.A., Samy, A.M., and Afouna, M.M. (2024). FORMULATION AND EVALUATION OF NANOSTRUCTURED LIPID CARRIERS LOADED WITH REPAGLINIDE. Al-Azhar Journal of Pharmaceutical Sciences *69*, 1-24.

Nirwan, N., Nikita, Sultana, Y., and Vohora, D. (2021). Liposomes as multifaceted delivery system in the treatment of osteoporosis. Expert Opinion on Drug Delivery *18*, 761-775.

Pandey, S., Patel, P., and Gupta, A. (2018). Novel solid lipid nanocarrier of glibenclamide: A factorial design approach with response surface methodology. Current Pharmaceutical Design *24*, 1811-1820.

Pandey, S.S., Patel, M.A., Desai, D.T., Patel, H.P., Gupta, A.R., Joshi, S.V., Shah, D.O., and Maulvi, F.A. (2020). Bioavailability enhancement of repaglinide from transdermally applied nanostructured lipid carrier gel: optimization, in vitro and in vivo studies. Journal of Drug Delivery Science and Technology *57*, 101731.

PATEL, M., and KHAN, M.A. (2023). OPTIMIZATION, DEVELOPMENT AND EVALUATION OF REPAGLINIDE CONTROLLED RELEASE GASTRO-RETENTIVE FLOATING TABLET USING CENTRAL COMPOSITE DESIGN. Int J App Pharm *15*, 218-226.

Patnaik, S., Gorain, B., Padhi, S., Choudhury, H., Gabr, G.A., Md, S., Mishra, D.K., and Kesharwani, P. (2021). Recent update of toxicity aspects of nanoparticulate systems for drug delivery. European Journal of Pharmaceutics and Biopharmaceutics *161*, 100-119.

Perrett, S., Golding, M., and Williams, W.P. (1991). A simple method for the preparation of liposomes for pharmaceutical applications: characterization of the liposomes. Journal of pharmacy and pharmacology *43*, 154-161.

Rahman, M.A., Ali, A., Rahamathulla, M., Salam, S., Hani, U., Wahab, S., Warsi, M.H., Yusuf, M., Ali, A., and Mittal, V. (2023). Fabrication of sustained release curcumin-loaded solid lipid nanoparticles (cur-SLNs) as a potential drug delivery system for the treatment of lung cancer: Optimization of formulation and in vitro biological evaluation. Polymers *15*, 542.

Rajan, R., Jose, S., Mukund, V.B., and Vasudevan, D.T. (2011). Transferosomes-A vesicular transdermal delivery system for enhanced drug permeation. Journal of advanced pharmaceutical Technology & Research *2*, 138-143.

Ramkanth, S., Chetty, C.M., Sudhakar, Y., Thiruvengadarajan, V., Anitha, P., and Gopinath, C. (2018). Development, characterization & invivo evaluation of proniosomal based transdermal delivery system of Atenolol. Future Journal of Pharmaceutical Sciences *4*, 80-87.

Sharma, D.S., Wadhwa, S., Gulati, M., Kumar, B., Chitranshi, N., Gupta, V.K., Alrouji, M., Alhajlah, S., AlOmeir, O., and Vishwas, S. (2023). Chitosan modified 5-fluorouracil nanostructured lipid carriers for treatment of diabetic retinopathy in rats: A new dimension to an anticancer drug. International journal of biological macromolecules *224*, 810-830.

Sharma, M., Kohli, S., and Dinda, A. (2015). In-vitro and in-vivo evaluation of repaglinide loaded floating microspheres prepared from different viscosity grades of HPMC polymer. Saudi pharmaceutical journal *23*, 675-682.

Singh, S., Vardhan, H., Kotla, N.G., Maddiboyina, B., Sharma, D., and Webster, T.J. (2016). The role of surfactants in the formulation of elastic liposomal gels containing a synthetic opioid analgesic. International journal of nanomedicine, 1475-1482.

Soni, N.K., Sonali, L., Singh, A., Mangla, B., Neupane, Y.R., and Kohli, K. (2020). Nanostructured lipid carrier potentiated oral delivery of raloxifene for breast cancer treatment. Nanotechnology *31*, 475101.

Srivastava, S., Mahor, A., Singh, G., Bansal, K., Singh, P.P., Gupta, R., Dutt, R., Alanazi, A.M., Khan, A.A., and Kesharwani, P. (2021). Formulation development, in vitro and in vivo evaluation of topical hydrogel formulation of econazole nitrate-loaded β-cyclodextrin nanosponges. Journal of Pharmaceutical Sciences *110*, 3702-3714.

Swidan, S.A., Mansour, Z.N., Mourad, Z.A., Elhesaisy, N.A., Mohamed, N.A., Bekheet, M.S., Badawy, M.A., Elsemeiri, M.M., Elrefaey, A.E., and Hassaneen, A.M. (2018). DOE, formulation, and optimization of Repaglinide nanostructured lipid carriers. Journal of Applied Pharmaceutical Science *8*, 008-016.

Tiss, M., and Hamden, K. (2022). Globularia alypum Extracts Attenuate Hyperglycemia and Protect against Various Organ Toxicities in Alloxan-Induced Experimental Diabetic Rats. Evidence-Based Complementary and Alternative Medicine *2022*.

Tupal, A., Sabzichi, M., Ramezani, F., Kouhsoltani, M., and Hamishehkar, H. (2016). Dermal delivery of doxorubicin-loaded solid lipid nanoparticles for the treatment of skin cancer. Journal of microencapsulation *33*, 372-380.

Wei, C.-C., and Ge, Z.-Q. (2012). Influence of electrolyte and poloxamer 188 on the aggregation kinetics of solid lipid nanoparticles (SLNs). Drug Development and Industrial Pharmacy *38*, 1084-1089.

Xinying, W., Peng, X., Mingbiao, X., Lei, P., and Yu, Z. (2023). Synergistic improvement of foam stability with SiO2 nanoparticles (SiO2-NPs) and different surfactants. Arabian Journal of Chemistry *16*, 104394.

Yu, G., Ali, Z., Khan, A.S., Ullah, K., Jamshaid, H., Zeb, A., Imran, M., Sarwar, S., Choi, H.-G., and ud Din, F. (2023). Preparation, Pharmacokinetics, and Antitumor Potential of Miltefosine-Loaded Nanostructured Lipid Carriers [Retraction]. International Journal of Nanomedicine *18*, 1107-1108.

Zhao, S., Yang, X., Garamus, V.M., Handge, U.A., Bérengère, L., Zhao, L., Salamon, G., Willumeit, R., Zou, A., and Fan, S. (2014). Mixture of nonionic/ionic surfactants for the formulation of nanostructured lipid carriers: effects on physical properties. Langmuir *30*, 6920-6928.

Zheng, H., Xu, C., Fei, Y., Wang, J., Yang, M., Fang, L., Wei, Y., Mu, C., Sheng, Y., and Li, F. (2020). Monoterpenes-containing PEGylated transfersomes for enhancing joint cavity drug delivery evidenced by CLSM and double-sited microdialysis. Materials Science and Engineering: C *113*, 110929.

تطوير وتوصيف البروترانسفرسومات المحملة بعقار نموذجي لتوصيله عبر الجلد

حاتم محمد توفيق حسن *[١،٣]، محمد أحمد نصر الدين اسماعيل [٣،٤]، محمد عبد المنعم عقل [٢]، محمد مصطفي السيد [١]، أحمد رفعت محمد جردوح [١]

[١]قسم الصيدلانيات والصيدلة الصناعية، كلية الصيدلة، جامعة قناة السويس، الإسماعيلية، ٤١٥٢٢، مصر.

[٢]قسم الصيدلانيات والتكنولوجيا الصيدلية، كلية الصيدلة (بنين)، جامعة الأزهر، ١ ش المخيم الدائم، مدينة نصر، ص.ب. صندوق بريد ١١٨٨٤، القاهرة، مصر.

[٣]الأكاديمية الطبية العسكرية.

[٤]مصنع انتاج الأدوية للقوات المسلحة

* البريد الالكتروني للباحث الرئيسي: hatemmohamedtawfek@yahoo.com

عقار الريباجلينيد هو دواء مضاد لمرض السكري من النوع الثانى ينتمي إلى فئة ميجليتينيد، والذي يتم تناوله عن طريق الفم ويستخدم لتحسين إفراز الأنسولين الناتج عن الوجبة. يتم التخلص منه بسرعة من الجسم عن طريق الإفراز الصفراوي. يخضع REP لعملية استقلاب واسعة النطاق للمرور الأول في الكبد، مما يؤدي بشكل إجمالي إلى ضعف التوافر الحيوي للدواء عن طريق الفم (٥٦%). يحتوي على نسبة عالية من الارتباط ببروتينات البلازما (أكثر من ٩٨%)، ويبلغ نصف عمره في الدورة الدموية الجهازية حوالي ساعة واحدة. يتمتع REP بقابلية ذوبان منخفضة جدًا في الماء (٣٤ ميكروغرام / مل عند ٣٧ درجة مئوية) وقابلية عالية للدهون كما أنه يعاني من توافر حيوي منخفض ومتغير. كان الهدف من هذه الدراسة هو تطوير نظام ناقل نانوي يسمى البروترانسفيرسومات المحملة برياجلينيد الذي يوفر فوائد إطلاق الدواء لفترة طويلة ويعزز توافره البيولوجي. تصنيع الحويصلات النانوية المحملة بـالريباجلينيد باستخدام أنواع مختلفة من المواد الخافضة للتوتر السطحي (توين ٨٠، اسبان ٦٠، بولوكسامير ١٨٨). تم تحضير جميع التركيبات (حويصلات البروترانسفيرسومات النانوية الستة المختلفة ذات منشط حافة مختلف وتم تحليلها لاحقًا من حيث الحجم والجهد السطحى للجزيئات وكذلك مؤشر تعدد التشتت وكفاءة تحميل العقار داخل الجزيئات النانوية المحضرة. أظهرت النتائج أن تغيير نوع المادة الخافضة للتوتر اسطحي كان له تأثير كبير على حجم الجسيمات، ومؤشر تعدد التشتت وسلوك إنطلاق العقار معمليا. كما أظهرت إنطلاقًا طويلًا للدواء مقارنة بالعقار نفسه دون اى إضافات. يتراوح متوسط حجم الجسيمات بين ١٨٤.٧ ± ٩.٧ الي ٦٢٩.٧ ± ١٧٢.٥ نانومتر. أظهرت الجسيمات شحنة سالبة، حيث تتراوح قيم زيتا المحتملة من . ٣٧.٧٧ ± ١.٧٧ إلى . ٢٩.١ ± ١.٠٣ مللي فولت. تراوحت نسبة التحميل بين ٧٨ ± ٤.٩ الي ٩٥.٨ ± ٣.٢٪. أظهرت الصيغة المثلى إطلاقًا طويلًا للدواء مقارنةً بذوبان بالعقار نفسه أدى التطبيق الموضعي لناقلات البروترانسفروسومات على جلد البطن لدى الفئران الخالية من الشعر إلى امتصاص الدواء بشكل أفضل مقارنة بالعقار نفسه دون اى إضافات. في الختام، تشير هذه النتائج إلى أن البروترانسفرسوم لديه القدرة على توصيل عقار ريباجلينيد عبر الجلد.

الكلمات المفتاحية : ريباجلينيد، البروترانسفيرسومات ، نظام التوصيل عبر الجلد – التوافر البيولوجي.